

Effect of suction on macular thickness and retinal nerve fiber layer thickness during LASIK used femtosecond laser and Moria M2 microkeratome

Jing Zhang, Yue-Hua Zhou

Ophthalmic Center, Beijing Key Laboratory of Ophthalmology and Visual Science, Beijing Tongren Hospital, Capital Medical University, Beijing 100730, China

Correspondence to: Yue-Hua Zhou. Ophthalmic Center, Beijing Tongren Hospital, No. 1 Dongjiaomin Ln, Dongcheng District, Beijing 100730, China. yh0220@yahoo.com

Received: 2014-07-30 Accepted: 2015-01-08

Abstract

• **AIM:** To compare the effect of suction on the macular thickness and retinal nerve fiber layer (RNFL) thickness during laser *in situ* keratomileusis (LASIK) used Ziemer FEMTO LDV femtosecond laser (Ziemer group) and Moria M2 automated microkeratome (Moria group) for flap creation.

• **METHODS:** Fourier -domain optical coherence tomography (FD-OCT) was used to measure macular thickness, ganglion cell complex thickness and RNFL thickness of 204 eyes of 102 patients with the Ziemer femtosecond laser (102 eyes) and the Moria M2 microkeratome (102 eyes) before surgery and 30min; 1, 3d; 1wk; 1, 3mo; 1y after surgery.

• **RESULTS:** The average foveal thickness and parafoveal retinal thickness 30min after the surgery were statistically more than that before surgery (Ziemer $P < 0.001$, $P = 0.003$ and Moria $P = 0.001$, $P = 0.006$) and the effect was less in the Ziemer group than that in the Moria group (P all < 0.05). The ganglion cell complex thickness was not significantly changed in both groups (P all > 0.05). The RNFL thickness was statistically less 30min after surgery in both groups ($P = 0.014$, $P < 0.001$), but the influence was less in Ziemer group than that in Moria group ($P = 0.038$). However, the RNFL thickness had recovered to the preoperative level only 1d after surgery.

• **CONCLUSION:** The suction of femtosecond laser and mechanical microkeratome led to the increase in macular central fovea thickness and the decrease in RNFL thickness values at the early stage after LASIK. The effect of suction on macular and the RNFL thicknesses in Ziemer group is smaller than that in Moria group.

• **KEYWORDS:** laser *in situ* keratomileusis; femtosecond laser; macular; retinal nerve fiber layer; optical coherence tomography

DOI:10.3980/j.issn.2222-3959.2015.04.24

Zhang J, Zhou YH. Effect of suction on macular thickness and retinal nerve fiber layer thickness during LASIK used femtosecond laser and Moria M2 microkeratome. *Int J Ophthalmol* 2015;8(4):777-783

INTRODUCTION

Femtosecond laser has a significant impact on refractive surgery by enabling nonmechanical creation of corneal flaps during laser *in situ* keratomileusis (LASIK). The femtosecond laser offers advantages over microkeratomes. These include increased precision, a reduced incidence of flap complications, and the ability to cut thinner flaps without the risk of buttonhole formation^[1-6]. During LASIK flap creation, intraocular pressure (IOP) increases to levels exceeding 65 mm Hg. Femtosecond laser flap creation exerts less extreme IOP fluctuations but requires more procedural time than when a microkeratome is used^[7-9]. The sudden spike in IOP, which can damage the eye, has been observed during LASIK^[10,11]. However, whether the sudden spike in IOP during femtosecond laser-assisted LASIK and automated microkeratome LASIK damages the retina requires further study. To our knowledge, there are no reports in the literature comparing the macular thickness and RNFL changes following the LASIK used femtosecond laser and mechanical microkeratome for flap creation.

The aim of this prospective study was to use Fourier-domain optical coherence tomography (OCT) (RTVue OCT-100, Optovue, Inc. Fremont, CA, USA) to evaluate and compare the effects of suction on the macular and the peripapillary retinal nerve fiber layer (RNFL) thickness during LASIK used Ziemer FEMTO LDV femtosecond laser (Ziemer Group, Switzerland) and Moria M2 automated microkeratome (Moria group, Antony, France) for flap creation.

SUBJECTS AND METHODS

Subjects Two hundred and four eyes of 102 patients who were consecutively scheduled for LASIK treatment from December 2009 to August 2010 in the Tongren Ophthalmic Center of Capital Medical University, were enrolled in this prospective study. All candidates had to be a minimum of 18y and were able to return to the center for one-year follow-up. The local ethics committee approved the study, and all patients informed consent.

All patients underwent a complete preoperative examination including uncorrected visual acuity (UCVA), best corrected visual acuity (BCVA), slitlamp examination, applanation tonometry, fundus biomicroscopy, manifest and cycloplegic

refraction, keratometry, ultrasonic pachymetry, corneal topography and indirect ophthalmoscopy.

Patients with ocular pathologies such as keratoconus, corneal scars, corneal dystrophies, previous ocular surgery, glaucoma, IOP>21 mm Hg, evidence of glaucomatous optic nerve damage, and cup-to-disc ratio>0.4, diabetes, or other systemic diseases known to affect the eye were excluded.

On the basis of the flap creation technique, 2 groups were formed. One group had femtosecond laser-assisted LASIK (Ziemer group) and the other, LASIK with microkeratome Moria M2 110 μm-head (Moria group).

Fourier –domain Optical Coherence Tomography Measurements

Macular and the peripapillary RNFL thickness measurements were performed by the same examiner (Zhang J) using the RTVue-100 OCT system (software version: 4.0.5.100), which is based Fourier-domain (FD) technology. The RTVue-100 has an axial resolution of 5 μm and acquires high-resolution images with 26 000 axial scans per second. The examinations were before surgery and 30min; 1, 3d; 1wk; 1, 3mo, 1y after surgery. The OCT measurements were performed without pupil dilation.

Macular thickness was measured using "MM6" mode, which is based on repeated A-scans arranged along 12 radial lines with a 6-mm scan length. Examinations were formed in the fovea, parafoveal and perifoveal zones according to the regions determined in ETDRS study (Early Treatment Diabetic Retinopathy Study Research Group 1985), and the average thickness is presented as numerical values or as a false color code for nine modified ETDRS areas (Figure 1). The thickness map represents the average thickness of fovea (1.0 mm diameter central circle area) and 3.0 mm parafoveal (ring area between 1 mm and 3 mm in diameter resulting in a 2.5 mm wide parafoveal ring) and 6.0 mm perifoveal (ring area between 3 mm and 6 mm in diameter resulting in a 3 mm wide perifoveal ring) regions divided into superior (S, 46°-135°), nasal (N, 136°-225°), inferior (I, 226°-315°) and temporal (T, 316°-45°) quadrants (Figure 1).

The ganglion cell complex was measured using the scan protocol "GCC". This protocol uses one horizontal line with a 7-mm scan length (467 axial scans per line, centered 1 mm temporal to the fovea) followed by 15 vertical lines with a 7-mm scan length (400 axial scans per line, 0.5-mm interval between two lines, centered in the middle of the horizontal scan line). The GCC thickness was measured from the internal limiting membrane to the inner plexiform layer boundary. The following GCC parameters were analyzed in this study: average thickness, thickness in the superior and inferior hemisphere.

The RNFL thickness was determined using the optic nerve head protocol. The protocol uses 13 concentric ring scans 1.3 to 4.9 mm in diameter (587 to 965 different axial scans per ring) centered in the optic disc. The RNFL thickness results were shown as thickness map of 16 regions (Figure 2).

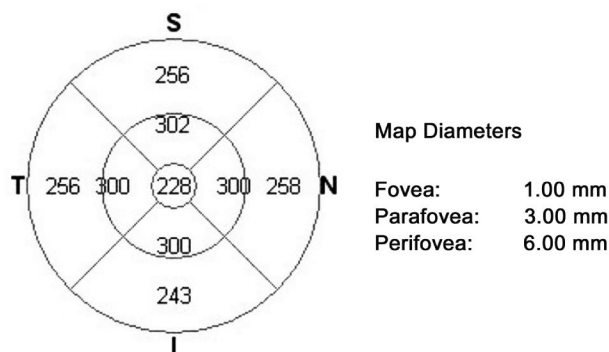


Figure 1 The nine macular areas defined by the Early Treatment Diabetic Retinopathy Study Research Group (1985).

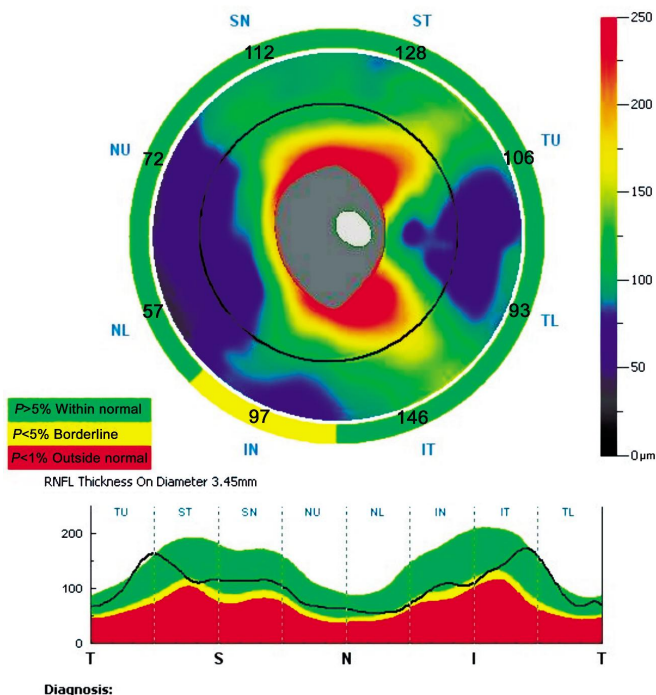


Figure 2 The retinal nerve fiber layer thickness was measured in 16 regions. Data obtained were compared with the normative database provided with the OCT software, taking the patient age and size of the optic disc into account.

The Signal Strength Index (SSI) was used to control for image quality. Images with a SSI less than 50 were excluded, and scans with movement or decentration artifacts were repeated. The results from the comparison of macular, GCC and RNFL thicknesses to normative data were illustrated with a stoplight color scheme for each protocol. Thicknesses in the normal range were represented by green areas, those that were abnormal at the 5% level were represented by yellow areas, and those that were abnormal at the 1% level were represented by red areas.

Surgical Procedure The same experienced surgeon (Zhou YH) performed all the LASIK procedures under topical anesthesia. The Ziemer femtosecond laser was programmed to a thickness of 110 μm and was used to create an 8.5 mm diameter corneal flap with the hinge placed superiorly. The laser energy was set at <10 nanojoule (nJ) pulse energy with a frequency higher than 5 MHz. The pulse duration was between 200 and 350 femtosecond. The line and spot separations were less than 2 μm.

The microkeratome Moria M2 110 μm -head (Moria M2) was used to created an 8.5 mm diameter corneal flap with a superior hinge. It was used to attempt a flap thickness of 110 μm based on previous experience.

After lifting the flap, ablations were performed using the Visx S4 excimer laser (VISX Inc., Santa Clara, USA) with a 6.0 mm optical zone and 0.5 mm transition zone. The corneal flap and stroma surface were irrigated with balanced normal saline solution, and the flap was repositioned. After the operation, patients were instructed to instill fluorometholone 0.1% four times per day for 3d, and then tapered over for two weeks, and levofloxacin and artificial tears four times per day for 2wk. All patients were asked to have regular follow-up visits, and postoperative examinations were performed at 30min; 1, 3d; 1wk; 1, 3, 6mo and 1y after surgery.

Statistical Analysis Statistical analysis was performed using SPSS software (version 17.0, SPSS Inc. Chicago, IL, USA). The thickness was compared between groups using an independent-samples *t* test. One-way analysis of variance (ANOVA) was used to analyze thickness between follow-up visits. The Wilcoxon signed-rank test was applied to identify measurement data not conforming to normal distribution. A *P* value less than 0.05 was considered statistically significant.

RESULTS

Participants Table 1 shows the preoperative characteristics of the patients. There were no statistically significant differences between Ziemer group and Moria group ($P>0.05$).

Macular Thickness Table 2 shows the macular thickness values before and after surgery. In Ziemer group, the average foveal and parafoveal retinal thicknesses 30min after the surgery ($243.19 \pm 25.51 \mu\text{m}$, $316.21 \pm 14.77 \mu\text{m}$) were significantly thicker than that before surgery ($238.62 \pm 26.58 \mu\text{m}$, $311.67 \pm 15.23 \mu\text{m}$, $P<0.001$, $P=0.003$, ANOVA), among that paratemporal and paranasal quadrants were changed significantly ($P=0.002$, $P=0.011$, ANOVA). However, the perifoveal retinal thickness was not changed significantly ($P=0.586$, ANOVA) 30min after surgery. One day, 3d; 1wk; 1, 3mo and 1y after surgery, the foveal, parafoveal and perifoveal retinal thicknesses were not changed significantly (P all >0.05 , ANOVA; Table 2).

In Moria group, the average foveal and parafoveal retinal thickness 30min after the surgery was significant thicker than that before surgery ($P=0.001$, $P=0.006$, ANOVA), among that the thickness of paratemporal, parasuperior and paranasal quadrants was also significant thicker than that preoperatively ($P=0.034$, $P=0.025$, $P=0.032$, ANOVA). However, the perifoveal retinal thickness was not changed significantly ($P=0.812$, ANOVA) 30min after the surgery. One day, 3d; 1wk; 1, 3mo and 1y after surgery, the averages of foveal, parafoveal and perifoveal retinal thicknesses were not changed significantly (P all >0.05 , ANOVA), but the paratemporal and paranasal quadrants were still significantly thicker 1d and 3d after surgery than that before surgery ($P=0.019$ - 0.038 , ANOVA).

Characteristics	Ziemer LDV	Moria M2	<i>n</i> (%)
No. of eyes	102	102	-
Age (a)	26.05±4.67	25.32±3.93	0.546
F	62 (60.8)	65(63.7)	0.789
Intraocular pressure (mm Hg)	15.64±3.87	14.89±3.58	0.753
Spherical equivalent (D)	-6.43±2.24	-5.93±1.95	0.436
Central Corneal Thickness (μm)	553.26±22.56	556.72±23.78	0.348
Corneal curvature (D)	44.46±1.89	43.66±1.54	0.637

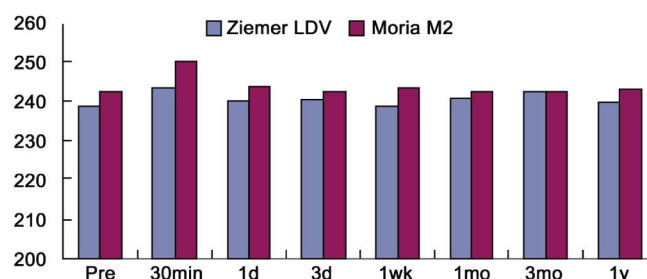


Figure 3 The average foveal retinal thickness values before and after surgery.

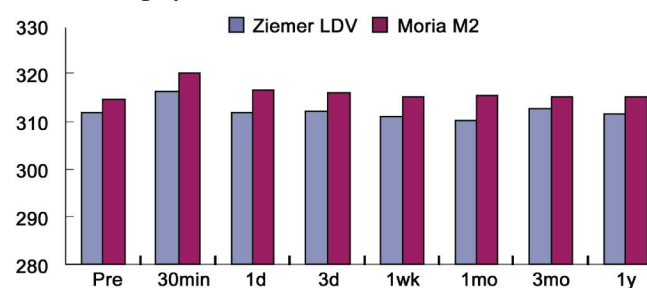


Figure 4 The average parafoveal retinal thickness values before and after surgery.

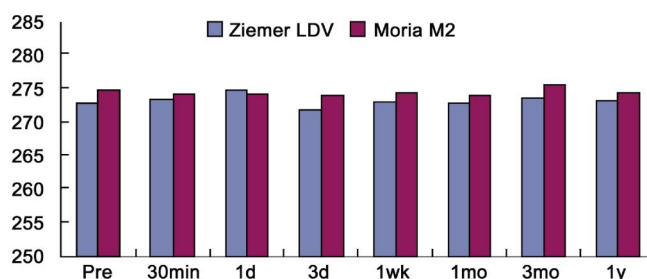


Figure 5 The perifoveal retinal thickness values before and after surgery.

The average foveal and parafoveal retinal thickness and parasuperior, paranasal retinal thickness in Moria group were statistically more than that in Ziemer group 30min after surgery (P all <0.05 , *t*-test for independent samples). However, the difference of the perifoveal retinal thickness between two groups was not significant (P all >0.05 , *t*-test for independent samples; Figures 3-5).

Perimacular Ganglion Cell Complex In both groups, the ganglion cell complex thickness, including average thickness, thickness in the superior and inferior hemisphere, was not significantly changed 30min; 1, 3d; 1wk; 1, 3mo and 1y compared with that preoperatively (P all >0.05 , ANOVA). The difference in the gaglion cell complex thickness between Ziemer group and Moria group was not statistically significant at any follow-up visits (P all >0.05 , ANOVA; Table 3).

Table 2 Macular thickness values before and after surgery (µm) n=102

Macular thickness	Pre-surgery	30min	1d	3d	1wk	1mo	3mo	1y
Ziemer LDV								
Fovea	238.62±26.58 ^a	243.19±25.51 ^{ab}	239.78±28.77	240.29±20.79	238.38±23.28	240.53±21.69	241.89±22.23	239.68±20.63
Parafovea	311.67±15.23 ^a	316.21±14.77 ^{ab}	311.74±14.32	312.10±12.93	311.02±13.56	310.33±13.07	312.64±14.38	311.51±13.15
Paratempo	307.39±15.41 ^a	314.76±20.72 ^a	309.46±16.42	307.46±14.58	306.82±14.18	306.49±14.18	306.98±13.33	307.63±13.15
Parasuperior	315.97±13.88	316.16±15.05 ^b	315.79±13.44	314.92±13.68	314.82±13.81	314.38±13.56	316.91±14.01	315.48±13.38
Paranasal	310.17±19.81 ^a	316.65±19.22 ^{ab}	311.85±16.93	311.71±13.88	309.98±14.32	309.65±13.02	311.94±16.64	311.25±13.16
Parainferior	313.14±16.06	314.27±15.42	313.89±15.65	314.33±13.82	313.47±14.97	313.79±13.54	314.57±17.25	313.28±14.87
Perifovea	272.63±13.62	273.20±13.23	274.55±13.55	271.88±16.64	272.89±12.86	272.57±13.15	273.38±17.63	273.14±12.88
Peritempo	273.48±15.29	272.75±20.19	274.76±15.68	271.88±16.64	272.89±12.86	274.04±13.98	274.53±21.01	273.64±13.26
Perisuperior	269.79±16.26	271.39±16.49	271.61±16.09	269.48±15.67	270.14±15.84	269.99±15.35	270.89±16.43	269.12±14.46
Perinasal	279.72±17.21	278.76±15.35	280.63±22.22	278.77±14.52	279.95±13.62	278.78±14.29	279.29±21.38	279.35±15.19
Periinferior	267.53±16.96	269.91±17.37	269.19±17.09	268.33±15.35	268.23±14.85	269.11±15.11	270.81±15.22	268.43±14.92
Moria M2								
Fovea	241.96±17.09 ^a	249.85±22.41 ^{ab}	243.55±21.48	241.95±17.51	243.12±20.36	242.02±19.72	241.96±14.49	242.74±14.89
Parafovea	314.71±15.86 ^a	320.21±15.97 ^{ab}	316.51±15.76	315.81±13.69	315.17±16.88	315.19±12.33	314.95±10.89	315.07±11.41
Paratempo	310.51±18.62 ^a	316.09±17.05 ^a	315.94±17.02 ^a	315.33±13.67 ^a	311.31±17.28	310.84±17.71	310.93±11.75	310.09±12.17
Parasuperior	319.21±18.82 ^a	326.59±16.21 ^{ab}	321.94±15.98	320.21±14.54	320.81±17.21	320.01±9.96	319.37±11.43	319.7111.43±
Paranasal	314.43±18.66 ^a	321.71±16.71 ^{ab}	319.04±17.26 ^a	318.76±14.43 ^a	316.1±17.82	314.32±17.81	313.13±11.36	313.05±12.09
Parainferior	314.73±12.94	314.71±15.71	314.84±15.19	313.92±14.13	314.39±17.04	314.61±10.71	315.39±11.29	315.41±12.37
Perifovea	274.44±14.93	274.15±14.24	274.02±15.29	273.93±13.12	274.37±16.09	273.96±11.23	275.39±8.42	274.29±9.74
Peritempo	274.37±18.75	274.07±16.89	275.71±16.08	274.05±13.24	274.41±17.31	274.81±14.59	274.97±9.16	275.72±10.98
Perisuperior	273.39±20.98	272.12±16.72	272.08±16.29	272.75±15.61	271.11±17.52	272.36±12.09	273.21±11.94	272.36±12.46
Perinasal	281.26±16.44	281.12±15.23	281.63±15.47	280.47±14.34	280.55±17.19	279.57±17.27	281.75±8.91	280.84±10.46
Periinferior	268.86±16.02	270.44±15.07	270.58±14.68	269.31±14.69	269.08±16.47	270.12±11.17	269.65±11.32	269.25±12.65

^aValue for comparing the thicknesses of different follow-up visits used ANOVA, $P<0.05$; ^bValue for comparing the thicknesses of Ziemer LDV and Moria M2 groups used independent samples t -test, $P<0.05$.

Table 3 Perimacular ganglion cell complex parameters (µm) n=102

Time	Ziemer LDV			Moria M2		
	Average	Superior	Inferior	Average	Superior	Inferior
Pre-surgery	93.59±6.26	93.79±6.86	93.44±6.19	94.39±7.19	93.96±7.64	94.91±7.46
30min	94.39±8.13	94.46±8.43	94.38±8.81	94.86±6.64	94.78±7.57	95.12±6.63
1d	93.89±6.67	93.60±6.36	93.78±7.79	94.74±7.25	94.34±7.77	95.06±7.45
3d	93.99±6.45	93.82±7.04	93.54±7.27	94.69±6.71	93.95±7.12	94.62±6.91
1wk	93.68±6.73	93.69±6.90	93.62±7.63	93.91±6.89	93.59±7.35	94.24±7.02
1mo	93.12±6.97	93.31±6.03	93.01±8.67	93.38±4.52	93.89±5.24	94.94±4.84
3mo	94.03±8.21	94.19±7.44	93.97±8.75	93.71±4.86	94.40±5.92	93.15±4.92
1y	93.54±7.45	93.79±7.14	93.33±8.49	93.81±6.05	93.95±6.50	93.71±6.35

Peripapillary Retinal Nerve Fiber Layer Thickness In Ziemer group, the RNFL thickness, including the average thickness, and SN1, SN2 and TL2 RNFL thickness 30min after surgery and the superior, SN1, SN2 and TL2 RNFL thickness 1d after surgery, was statistically less than that before surgery (P all <0.05 , ANOVA). The difference in the RNFL thickness was not statistically significant at 3d, 1wk, 1mo, 3mo and 1y after surgery (P all >0.05 , ANOVA; Table 4).

In Moria group, the RNFL thickness, including the average, temporal, superior and TU2, ST2, IT2, TL2, TL1 RNFL

thickness 30min after surgery was significantly less than that preoperatively (P all <0.05 , ANOVA). The difference in the RNFL thickness was not statistically significant at 1, 3d; 1wk; 1, 3mo and 1y after surgery (P all >0.05 , ANOVA; Table 4). The temporal RNFL thickness in Moria group was significantly less than that in Ziemer group 30min after surgery ($P=0.038$, t -test for independent samples). The difference in the RNFL thickness was not statistically significant between 2 groups preoperatively and at 1, 3d; 1wk; 1, 3mo and 1y after surgery (P all >0.05 , t -test for independent samples; Table 4).

Table 4 Peripapillary retinal nerve fibre layer thickness (µm)

RNFL	Pre-surgery	30min	1d	3d	1wk	1mo	3mo	1y
<i>n</i> =102								
Ziemer LDV								
Average	106.06±9.70 ^a	104.17±9.31 ^a	105.80±9.67	106.25±9.94	105.96±9.29	105.68±12.74	105.83±15.98	105.49±10.09
Tempo	89.08±14.94	89.81±14.04 ^b	88.84±13.43	89.01±15.73	89.01±14.06	88.99±21.84	89.13±20.77	89.35±17.11
Superior	128.97±17.73 ^a	127.79±17.73	126.88±18.82 ^a	128.29±19.48	128.92±19.16	128.29±20.78	128.88±19.71	127.62±20.09
Nasal	71.12±16.73	70.67±16.92	71.86±16.34	71.52±17.09	71.38±16.01	71.67±14.39	71.09±17.42	71.87±12.27
Inferior	135.06±14.52	134.39±15.56	135.99±15.76	135.29±14.27	135.08±16.22	135.15±21.83	135.41±22.75	135.19±16.21
TU1	78.59±16.27	79.82±15.93	79.47±15.21	79.24±15.85	78.50±13.81	78.54±22.57	78.93±24.95	78.26±16.69
TU2	107.78±19.95	107.23±19.57	108.31±19.33	108.68±22.85	107.95±20.03	108.76±26.11	108.05±23.17	107.31±23.64
ST2	140.99±20.95	141.49±22.36	139.40±22.29	139.09±24.51	142.39±22.40	140.04±21.61	139.98±27.50	140.13±22.16
ST1	131.72±27.10	132.21±27.69	129.68±27.69	132.86±28.41	134.19±28.57	131.68±28.13	131.40±28.46	131.93±28.15
SN1	122.65±24.79 ^a	119.72±23.19 ^a	120.32±25.93 ^a	121.13±27.13	124.16±27.27	122.48±28.41	122.34±24.90	122.35±27.99
SN2	120.61±23.38 ^a	117.86±22.08 ^a	118.21±22.42 ^a	120.14±24.52	119.06±22.76	119.07±23.58	120.34±20.55	119.74±23.76
NU2	89.19±22.47	87.21±23.05	89.40±23.37	90.52±23.14	89.15±24.54	89.86±19.43	89.44±23.32	89.40±18.84
NU1	61.03±15.23	61.72±16.68	62.37±14.71	62.54±15.51	61.02±15.23	61.95±12.59	61.42±17.78	61.87±11.79
NL1	57.61±13.74	58.16±15.80	58.80±14.99	58.82±14.02	58.01±14.68	57.45±11.02	57.13±14.37	57.19±11.06
NL2	76.71±20.08	75.67±20.42	76.92±20.74	78.30±20.49	76.84±17.94	76.45±20.28	76.46±18.25	76.67±15.89
IN2	108.84±19.59	108.59±20.58	111.12±22.81	109.98±19.63	108.73±19.76	109.62±24.51	108.81±20.15	108.39±18.13
IN1	128.92±23.24	128.63±24.64	130.82±27.45	129.44±24.58	128.70±25.48	128.20±30.61	129.41±27.48	128.71±23.56
IT1	153.36±22.35	153.78±24.66	155.29±23.18	154.22±23.63	152.51±26.73	153.15±32.32	152.48±35.94	152.65±27.35
IT2	148.99±24.48	146.44±23.70	146.65±23.58	147.42±24.44	148.08±24.27	148.16±34.35	148.74±30.37	148.91±26.09
TL2	98.89±21.55 ^a	94.85±19.56 ^a	95.16±19.34 ^a	99.62±22.27	98.89±21.59	98.82±29.19	98.12±22.02	98.19±23.09
TL1	71.04±12.61	69.32±12.68	70.96±11.22	72.38±13.64	71.68±12.09	71.21±12.89	71.08±15.78	71.62±14.25
Moria M2								
Average	107.10±10.68 ^a	105.07±9.78 ^a	107.41±10.13	107.54±9.72	107.19±9.62	106.95±8.13	107.15±7.22	107.41±9.13
Tempo	87.83±14.98 ^a	84.45±13.24 ^{ab}	87.24±15.38	88.01±14.47	87.63±15.10	87.72±14.64	87.03±12.00	87.13±13.28
Superior	128.11±13.84 ^a	124.78±14.12 ^a	128.38±15.76	128.35±15.79	128.12±16.56	127.80±17.65	129.03±15.31	129.24±18.19
Nasal	72.69±13.97	71.83±11.83	73.09±14.21	72.99±12.48	72.87±12.44	72.58±14.69	72.44±12.18	72.09±12.00
Inferior	139.78±21.62	138.23±19.44	139.54±19.34	140.16±19.96	140.05±18.37	138.93±17.22	140.01±16.35	139.47±20.64
TU1	77.62±13.08	75.76±15.69	77.46±15.35	78.48±12.94	78.68±12.82	78.77±14.31	77.82±14.67	77.49±14.02
TU2	106.97±21.71 ^a	102.40±19.69 ^a	106.54±22.83	107.09±23.38	108.35±23.68	108.39±20.84	106.52±20.71	108.28±19.54
ST2	142.73±25.67 ^a	137.23±22.46 ^a	140.97±21.96	141.88±21.87	141.49±22.78	141.75±21.18	143.94±17.60	141.85±22.97
ST1	135.32±26.75	133.57±27.56	135.16±25.93	136.66±25.56	135.15±25.63	135.22±28.51	135.46±24.87	134.54±26.59
SN1	118.67±21.64	116.42±20.50	119.25±20.65	118.74±21.76	119.20±22.92	118.43±21.97	118.12±19.27	118.73±21.49
SN2	115.76±17.67	115.95±16.44	118.20±20.84	117.12±17.16	116.73±17.14	117.13±19.62	117.50±19.27	117.23±19.37
NU2	89.38±18.53	88.41±17.09	90.68±24.22	88.67±16.68	88.06±16.97	89.87±19.12	88.72±17.69	88.88±16.89
NU1	62.60±13.46	61.40±10.95	62.67±13.34	62.64±11.67	62.08±12.34	63.62±15.14	62.88±12.11	61.92±12.25
NL1	59.20±12.96	58.15±9.84	60.09±10.98	59.80±10.84	58.75±10.34	59.45±12.86	58.51±10.71	59.27±10.64
NL2	79.65±17.59	79.42±15.36	80.59±15.74	80.93±15.94	78.35±16.21	79.44±16.75	79.72±13.26	79.51±14.57
IN2	114.77±26.04	114.21±20.49	115.34±20.96	115.41±22.04	113.55±19.91	114.84±21.13	114.31±19.01	113.95±19.91
IN1	135.86±31.58	135.73±26.15	135.31±30.29	136.56±27.19	136.05±25.04	135.11±28.34	135.80±27.29	135.33±30.32
IT1	161.19±30.29	160.42±29.22	162.31±29.34	161.70±28.18	161.96±26.83	160.87±26.15	160.39±23.48	160.74±31.82
IT2	147.26±24.31 ^a	142.54±23.43 ^a	147.57±24.30	148.51±24.63	148.95±25.34	148.84±25.32	149.39±23.48	148.62±25.78
TL2	95.70±20.54 ^a	90.41±16.41 ^a	95.23±19.12	95.63±19.22	96.28±20.84	95.59±20.43	95.58±14.21	96.44±18.59
TL1	70.99±12.10 ^a	69.17±11.62 ^a	69.71±11.96	70.79±10.03	71.17±10.79	70.25±10.88	70.13±7.68	70.30±10.86

^aValue for comparing the thicknesses of different follow-up visits used ANOVA, *P*<0.05; ^bValue for comparing the thicknesses of Ziemer LDV and Moria M2 groups used independent samples *t*-test, *P*<0.05.

DISCUSSION

During LASIK, a suction ring applied to the anterior segment of the eye elevates the IOP to levels exceeding 65 mm Hg or more pressure during the application of suction. After

stopping the vacuum suction, IOP drops to normal, even more 5 mm Hg lower than before suction. The US Food and Drug Administration reports a complication rate of 1% to 5% after LASIK^[12]. Rare but devastating complications of LASIK

surgery involve the occurrence of posterior segment damage during the LASIK procedure, relating to the sudden strike in IOP during the flap creation causing rhegmatogenous events or damage to retinal ganglion cells, resulting in visual field defects^[13-16]. Recently, researchers reported that the maximum IOP levels were lower in the femtosecond laser group, while the duration of the suction phase was longer than that in the microkeratome group^[17-20]. Compared to microkeratome, the effect of femtosecond laser on optic nerve and RNFL thickness caused the ophthalmologists' widespread concern. Increased IOP is considered one of the major risk factors for the development, progression, and evaluation of glaucoma. The potential long term damage to the eye caused by the sudden spike in IOP observed during surgery^[21-23] is necessitated further investigation.

Thus, we performed this prospective clinical study of patients treated for myopia or myopic astigmatism. We used RTVue-100 OCT system to compare the effect of suction on the macular thickness, ganglion cell complex, and the peripapillary RNFL during femtosecond laser-assisted LASIK and LASIK with microkeratome. To our knowledge, this appears to be the first published study with long follow-up (1y) to use Fourier-domain OCT to compare the effect of suction on the retina during LASIK using the two major forms of flap creation, a microkeratome or a femtosecond laser.

Because LASIK alters corneal curvature and thickness, the normative parameters of conventional glaucoma screening tools are being questioned^[24]. The ability of OCT to assess retinal damage with measurements of the optic nerve head, the RNFL, and macular thickness has been demonstrated^[25,26]. Macular ganglion cell complex thickness measure by Fourier-domain OCT may be a good alternative or complementary to RNFL thickness and macular thickness assessment for detecting retinal damage in patients after LASIK^[27].

In this study, the average foveal and parafoveal retinal thicknesses statistically increased 30min after the surgery, while the perifoveal retinal thickness was not changed significantly in the both groups. The average foveal and parafoveal retinal thickness and parasuperior, paranasal retinal thickness in the Moria group were significantly thicker than that in Ziemer group 30min after surgery. The foveal, parafoveal and perifoveal retinal thicknesses were not changed significantly both in two groups 1d, 3d, 1wk, 1mo, 3mo and 1y after surgery. We speculate that the suction during femtosecond laser-assisted LASIK and LASIK used microkeratome might have caused slight localized edema of the macula early after surgery, mainly in the foveal, parafoveal retinal regions, while the perifoveal retina was not affected. The effect on the macular thickness was slighter in femtosecond laser than microkeratome. One day after

LASIK, the macular edema caused by the suction in LASIK used femtosecond laser and microkeratome had been recovered to the preoperative level.

The ganglion cell complex thickness did not significantly change in either groups. We hypothesize that the slight localized edema of the macula did not spread to the inner retina, which extends from the internal limiting membrane to the inner nuclear layer and includes the ganglion cell layer.

The effect of LASIK on RNFL thickness remains a matter of debates^[10,11,28-30]. Some studies reported LASIK did not significantly affect the RNFL parameters postoperatively^[10,11,28] while few studies found that RNFL thickness might decrease during uncomplicated LASIK^[29,30]. In our study, the RNFL thickness 30min after surgery was less than before surgery in both groups, and changes were less in the femtosecond laser group than in the microkeratome group. But this might not be of significance and is unlikely to have clinical consequences, because the corneal edema may affect the image quality of examination results 30min after surgery. Moreover, the RNFL thickness had recovered to the preoperative level only 1d after surgery. One of the interpretations about these results is that our study first proposed to measure the RNFL thickness 30min after surgery. Second, we used Fourier-domain OCT, which acquires high-resolution images with 26 000 axial scans per second and can detect changes of 5 μm magnitude. Other reasons were as follows: 1) The suction during surgery effects on retinal microcirculation. Research shows that whenever the IOP rise 10 mm Hg, the surrounding blood flow of optical disc decreases 7.4%-8.4%. Instantaneous changes of suction may cause ischemia-reperfusion injury. 2) The suction during surgery caused mechanical stretch to the retina. Sudden changes of IOP may cause mechanical stretch to vitreous base, and then cause posterior vitreous detachment, even retinal detachment. 3) The suction during surgery may cause disorder of optic nerve axoplasm, axon flow. High IOP can cause retinal ischemia, and axoplasm flow transport blocked in the sieve, malnutrition of retinal ganglion cells, so the RNFL thickness was thinning and defected. While the effect was transient and reversible, so the RNFL thickness thinning reverted to regain pre-operative thickness at day 1 after surgery.

In conclusion, slight localized edema of macula and reduction of the RNFL thickness were caused by LASIK using the two major forms of flap creation, namely a microkeratome or a femtosecond laser. While the changes were less in femtosecond laser group than those in the microkeratome group. Meanwhile, this effect was transient and reversible, because the macular thickness and the RNFL thickness recovered to the preoperative level only 1d after surgery. So the surgery of LASIK is safe and efficient, but surgeons should choose effective and safe suction mode, shorten the suction time and exclude potential retinopathy

and preexisting glaucoma before surgery to improve the safety and efficacy of LASIK.

ACKNOWLEDGEMENTS

Conflicts of Interest: Zhang J, None; Zhou YH, None.

REFERENCES

- 1 Diekmann H, Fischer D. Glaucoma and optic nerve repair. *Cell Tissue Res* 2013;353(2):327-337
- 2 Vidal-Sanz M, Salinas-Navarro M, Nadal-Nicolas FM, Alarcon-Martinez L, Valiente-Soriano FJ, de Imperial JM, Aviles-Trigueros M, Agudo-Barriuso M, Villegas-Perez MP. Understanding glaucomatous damage: anatomical and functional data from ocular hypertensive rodent retinas. *Prog Retin Eye Res* 2012;31(1):1-27
- 3 Kaneda M. Signal processing in the mammalian retina. *J Nippon Med Sch* 2013;80(1):16-24
- 4 Agudo-Barriuso M, Villegas-Perez MP, de Imperial JM, Vidal-Sanz M. Anatomical and functional damage in experimental glaucoma. *Curr Opin Pharmacol* 2013;13(1):5-11
- 5 Galindo-Romero C, Jimenez-Lopez M, Garcia-Ayuso D, Salinas-Navarro M, Nadal-Nicolas FM, Agudo-Barriuso M, Villegas-Perez MP, Aviles-Trigueros M, Vidal-Sanz M. Number and spatial distribution of intrinsically photosensitive retinal ganglion cells in the adult albino rat. *Exp Eye Res* 2013;108:84-93
- 6 Samuel MA, Zhang Y, Meister M, Sanes JR. Age-related alterations in neurons of the mouse retina. *J Neurosci* 2011;31(44):16033-16044
- 7 Schlamp CL, Montgomery AD, Mac Nair CE, Schuart C, Willmer DJ, Nickells RW. Evaluation of the percentage of ganglion cells in the ganglion cell layer of the rodent retina. *Mol Vis* 2013;19:1387-1396
- 8 Leung CK, Weinreb RN. Experimental detection of retinal ganglion cell damage in vivo. *Exp Eye Res* 2009;88(4):831-836
- 9 Gaillard F, Karten HJ, Sauve Y. Retinorecipient areas in the diurnal murine rodent *Arvicantha niloticus*: A disproportionately large superior colliculus. *J Comp Neurol* 2013;521(8):Spc1
- 10 Cao J, Naito J, Chen Y. Retrograde tracing with fluorescent microspheres reveals bifurcating projections from central retina to tectum and thalamus in chicks. *Anat Histol Embryol* 2012;41(4):306-310
- 11 Chiu K, Lau WM, Yeung S, Chang RC, So KF. Retrograde Labeling of Retinal Ganglion Cells by Application of Fluoro-Gold on the Surface of Superior Colliculus. *J Vis Exp* 2008;(16): pii:819
- 12 Huang TL, Huang SP, Chang CH, Lin KH, Sheu MM, Tsai RK. Factors Influencing the Retrograde Labeling of Retinal Ganglion Cells with Fluorogold in an Animal Optic Nerve Crush Model. *Ophthalmic Res* 2014; 51(4):173-178
- 13 Takihara Y, Inatani M, Hayashi H, Adachi N, Iwao K, Inoue T, Iwao M, Tanihara H. Dynamic imaging of axonal transport in living retinal ganglion cells in vitro. *Invest Ophthalmol Vis Sci* 2011;52(6):3039-3045
- 14 Yu DY, Cringle SJ, Balaratnasingam C, Morgan WH, Yu PK, Su EN. Retinal ganglion cells: Energetics, compartmentation, axonal transport, cytoskeletons and vulnerability. *Prog Retin Eye Res* 2013;36:217-246
- 15 Chidlow G, Ebnetter A, Wood JPM, Casson RJ. The optic nerve head is the site of axonal transport disruption, axonal cytoskeleton damage and putative axonal regeneration failure in a rat model of glaucoma. *Acta Neuropathol* 2011;121(6):737-751
- 16 Salinas-Navarro M, Alarcon-Martinez L, Valiente-Soriano FJ, Jimenez-Lopez M, Mayor-Torroglosa S, Aviles-Trigueros M, Villegas-Perez MP, Vidal-Sanz M. Ocular hypertension impairs optic nerve axonal transport leading to progressive retinal ganglion cell degeneration. *Exp Eye Res* 2010;90(1):168-183
- 17 Abbott CJ, Choe TE, Lusardi TA, Burgoyne CF, Wang L, Fortune B. Evaluation of retinal nerve fiber layer thickness and axonal transport 1 and 2wk after 8h of acute intraocular pressure elevation in rats. *Invest Ophthalmol Vis Sci* 2014;55(2):674-687
- 18 Huang W, Fileta J, Guo Y, Grosskreutz CL. Downregulation of Thy1 in retinal ganglion cells in experimental glaucoma. *Curr Eye Res* 2006;31(3): 265-271
- 19 Levkovitch-Verbin H, Makarovskiy D, Vander S. Comparison between axonal and retinal ganglion cell gene expression in various optic nerve injuries including glaucoma. *Mol Vis* 2013;19:2526-2541
- 20 Schlamp CL, Johnson EC, Li Y, Morrison JC, Nickells RW. Changes in Thy1 gene expression associated with damaged retinal ganglion cells. *Mol Vis* 2001;7:192-201
- 21 Nadal-Nicolas FM, Jimenez-Lopez M, Salinas-Navarro M, Sobrado-Calvo P, Albuquerque-Bejar JJ, Vidal-Sanz M, et al. Whole number, distribution and co-expression of brn3 transcription factors in retinal ganglion cells of adult albino and pigmented rats. *PLoS One* 2012;7 (11):e49830
- 22 Nadal-Nicolas FM, Jimenez-Lopez M, Sobrado-Calvo P, Nieto-Lopez L, Canovas-Martinez I, Salinas-Navarro M, Vidal-Sanz M, Agudo M. Brn3a as a marker of retinal ganglion cells: qualitative and quantitative time course studies in naive and optic nerve-injured retinas. *Invest Ophthalmol Vis Sci* 2009;50(8):3860-3868
- 23 Piri N, Kwong JM, Song M, Caprioli J. Expression of hermes gene is restricted to the ganglion cells in the retina. *Neurosci Lett* 2006;405(1-2): 40-45
- 24 Sanchez-Migallon MC, Nadal-Nicolas FM, Jimenez-Lopez M, Sobrado-Calvo P, Vidal-Sanz M, Agudo-Barriuso M. Brain derived neurotrophic factor maintains Brn3a expression in axotomized rat retinal ganglion cells. *Exp Eye Res* 2011;92(4):260-267
- 25 Gutierrez C, McNally M, Canto-Soler MV. Cytoskeleton proteins previously considered exclusive to ganglion cells are transiently expressed by all retinal neuronal precursors. *BMC Dev Biol* 2011;11:46
- 26 Chidlow G, Osborne NN. Rat retinal ganglion cell loss caused by kainate, NMDA and ischemia correlates with a reduction in mRNA and protein of Thy-1 and neurofilament light. *Brain Res* 2003;963(1-2): 298-306
- 27 Raymond ID, Pool AL, Vila A, Brecha NC. A Thy1-CFP DBA/2J mouse line with cyan fluorescent protein expression in retinal ganglion cells. *Vis Neurosci* 2009;26(5-6):453-465
- 28 Raymond ID, Vila A, Huynh U-CN, Brecha NC. Cyan fluorescent protein expression in ganglion and amacrine cells in a thy1-CFP transgenic mouse retina. *Mol Vis* 2008;14:1559-1574
- 29 Xu SY, Wu YM, Ji Z, Gao XY, Pan SY. A modified technique for culturing primary fetal rat cortical neurons. *J Biomed Biotechnol* 2012; 2012:803930
- 30 Sharma RK, Netland PA. Early born lineage of retinal neurons express class III beta-tubulin isotype. *Brain Res* 2007;1176:11-17